BEAM PHYSICS DESIGN OF THE INJECTOR FOR THE JAEA-ADS

B. Yee-Rendon*, Y. Kondo, J. Tamura, S. Meigo, F. Maekawa
Japan Atomic Energy Agency (JAEA), Tokai, Japan

Abstract

Accelerator-Driven Systems (ADS) represent an efficient solution to the challenge of nuclear waste disposal. Therefore, the Japan Atomic Energy Agency (JAEA) is designing a 30-MW proton linac as a key element of its proposal for the use of ADS technology. A key feature of ADS accelerators is their extremely high availability and reliability that is required to avoid thermal stress on reactor structures. To this end, JAEA-ADS adopted a combined strategy of hot standby in the front part of the linac and standby element compensation as a fast and efficient way to reduce the downtime due to an element failure. The JAEA-ADS injector is mainly composed of a normal conducting section and ends with the first section of superconducting cavities (Half-Wave Resonator). This paper presents the details of the optics design of the JAEA-ADS injector and the results of beam dynamics simulations.

INTRODUCTION

The Japan Atomic Energy Agency (JAEA) is developing an accelerator-driven subcritical system (ADS) aimed at the transmutation of minor actinides [1]. JAEA proposes the use of a 30-MW proton beam to generate spallation neutrons for an 800-MWth thermal power subcritical reactor, Table 1.

Table 1: Main Parameters for the JAEA-ADS Linac

Parameter		Trip duration
Beam current (mA)	20	
Proton beam energy (GeV)	1.5	
Duty factor (%)	100 (cw)	
RF frequency (MHz)	162/324/648	
Beam loss (W/m)	<1	
Beam trips per year [2]	2×10^4	≤10 s
	2×10^3	from 10 s to 5 min
	42	>5 min

ADS linacs demand a severe control over both the beam duration and the number of beam trips to prevent thermal stress on the reactor [2]. To achieve this, the JAEA-ADS linac implements a hybrid redundancy policy. This policy features a hot standby mode for the low-energy section and fast element compensation for the high-energy section [3], as shown in Fig. 1. The introduction of a hot standby creates new challenges in beam dynamics, particularly for beam transport, operation, and physical space. As a result, this paper presents and discusses an injector design that meets these requirements.

* byee@post.j-parc.jp

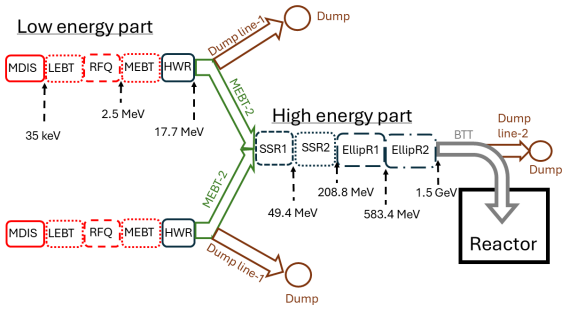

Figure 1: Schematic design of the linac for the JAEA-ADS.

DESIGN CONSIDERATIONS

The design of the proposed ADS linac for JAEA is nearly complete [4]. However, adopting the hot standby mode requires rethinking the injector design and its operation. Below, we discussed the considerations and proposed strategies to overcome them.

Low Beam Loss Control: < 1 W/m

Injector design should prioritize controlling emittance growth to reduce beam loss. This includes employing space charge compensation strategies, minimizing mismatches, and implementing achromatic bending to efficiently transport the beam to the high-energy section of the linac.

Transverse Space for Shielding

To ensure sufficient spacing between the two injectors, a distance greater than 4 m is recommended. Achieving this requires balancing bending angle, transport length, and beam loss.

High Beam Power Dump

In hot standby mode, the system is expected to operate as similarly to its primary part, producing a high beam power of 354 kW. This level of power presents significant challenges for the design of dump and shielding regarding an acceptable peak power density and the integral power. However, these issues can be addressed through pulse mode operation. In this mode, 99.5% of the beam is stopped by the chopper and collimator in the LEBT system, see Fig. 8. This results in approximately 800 W at a peak power density of 2 kW/cm^2, which is several order of magnitude lower than the scraper limit of the J-PARC linac's MEBT. Only 0.5% of the beam,1.7 kW, reaches the dump section. Thus, the beam dump requirements will be a peak power density of a few W/cm^2 and an integral beam power of a few kW. The pulse length corresponding to the 0.5% transmission is adequate for operation at nominal peak current. Consequently, the linac components in hot standby mode can be tuned to their

nominal current and repetition rate, allowing for a fast and safe ramping to full beam power by increasing the pulse length with the chopper. By selecting a reasonably lower-power beam for the hot standby part, the failure rate of the beam dump can be minimized.

LAYOUT

The injector layout is presented in Fig. 2. The injector starts with a microwave discharge ion source (MDIS) that provides a 25-mA proton beam with an energy of 35 keV. The proton is transported to the low-energy beam transport (LEBT) system. The beam is then accelerated by a 162-MHz RFQ to an energy level of 2.5 MeV. The medium-energy beam transport (MEBT) system carries the beam to the 162-MHz single-cell half-wave resonator (HWR) section, the first section of the superconducting linac. The section that connects the HWR with the 324 −MHz single spoke resonator (SSR1) section, which is the initial part of the high-energy section, is called MEBT-2. Additionally, there is a transport line called Dump line-1, which is used to dump the beam when this section operates in hot standby mode. In the next subsections, a description of the different section is provided.

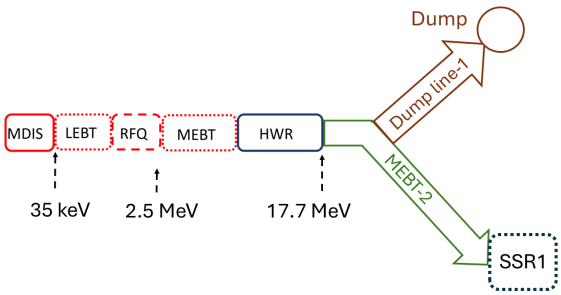

Figure 2: Layout of the injector part for the JAEA-ADS.

MDIS

Ion sources, basically, consist of a plasma generator and an extraction system. The plasma generator produces the necessary ions, while the extraction system configures the beam to the required size and orientation for the next stages. The extraction system has been reported previously [5]. A triode configuration was chosen as a balance of performance and simplicity.

LEBT

LEBT employs a magnetostatic design that utilizes space-charge compensation to reduce emittance growth [6–8]. The system includes two solenoids, a chopper, conical collimators, and beam diagnostics, Fig. 8-(a).

RFQ

The RFQ operates at a relatively low frequency of 162 MHz, which helps reduce the likelihood of inter-blade discharge and enhances operational availability. This lower frequency also minimizes heat dissipation, resulting in higher efficiency [9]. The RFQ utilizes a conventional design approach, employing the RFQuick code [10] developed by Los Alamos National Laboratory.

MEBT

The MEBT employs a compact and regular optical design that ensures uniform focusing in all directions [4]. Additionally, it is equipped with essential diagnostic elements for beam adjustment. To enhance beam quality in the downstream sections, the system includes six quadrupoles, two bunchers, four scrapers, and various beam diagnostic systems, as displayed in Fig. 3. The collimators removed large halo produced upstream to avoid potential losses in the superconducting section.

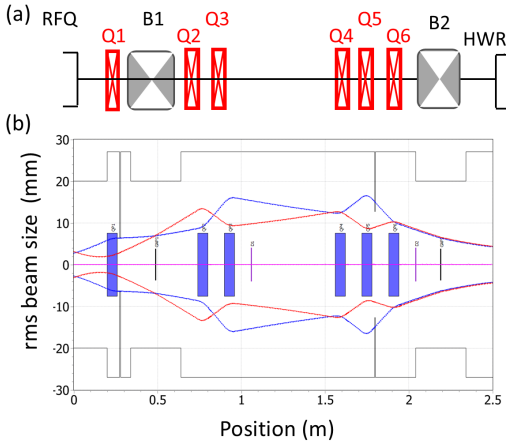

Figure 3: MEBT layout. Figure (a) shows the schematic and (b) the rms transverse envelopes.

HWR

The HWR section is the first superconducting part of the linac, designed to accelerate the beam from 2.5 MeV to 17.7 MeV. This section is made up of 25 periods, each consisting of a solenoid and an HWR cavity, as illustrated in Fig. 4.

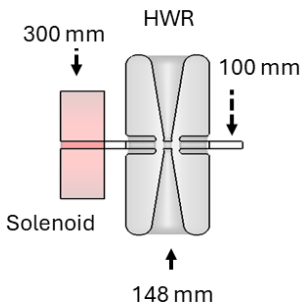

Figure 4: HWR lattice period. Theres is a 100 mm drift space between the solenoid and the HWR cavity.

At low energy, it is crucial to maintain periodicity to prevent emittance growth caused by mismatch. However, if all the periods were placed in a single cryomodule, it would be excessively large, approximately 18 m, which presents significant engineering challenge. To address this, the sections have been divided into three cryomodules: one containing nine periods and the other two containing eight periods each.

MEBT-2

MEBT-2 will begin with a matching section made up of triplet quadrupoles, which will help adjust the transverse beam size. This section will also include two normally conducting bunching cavities to control the bunch length. Following this, there will be an achromatic bending section composed of two 45−deg switched dipoles , accompanied by four superconducting solenoids. These solenoids are the same type to those used in the HWR and SSR sections. A modified cryomodule, of 2.8 m length, will be employed to house the solenoids. Figure 5 shows the rms transverse size, while Table 2 provides a summary of the elements in the MEBT-2 section. The total length is about 7 m and the transverse distance of 5.4 m. Similar design are used for other ADS linacs [11, 12], however they used normal quadrupoles inside the achromatic bending.

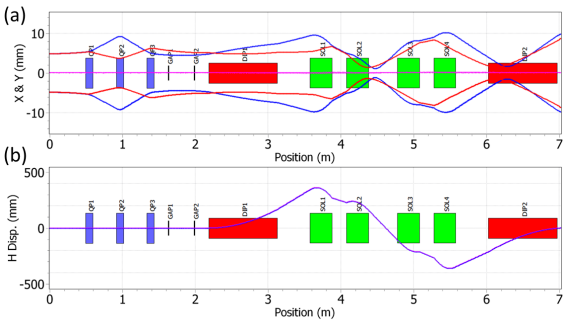

Figure 5: 3-σ rms transverse size on the top and the horizontal dispersion function along the MEBT-2.

Table 2: Main parameters of the MEBT-2. QP stands for quadrupole, Gap for buncher cavity, DIP for double switch dipole, and SOL for solenoid.

Element	length (mm)	Magnet Gradient (T/m) / Voltage (kV) / Field (T)
QP1	100	-7.9
QP2	100	14.3
QP3	100	-10.2
Gap1 & Gap2	300	145
DIP1 & DIP2	942	0.5
SOL1 & SOL4	300	2.9
SOL2 & SOL3	300	-2.8

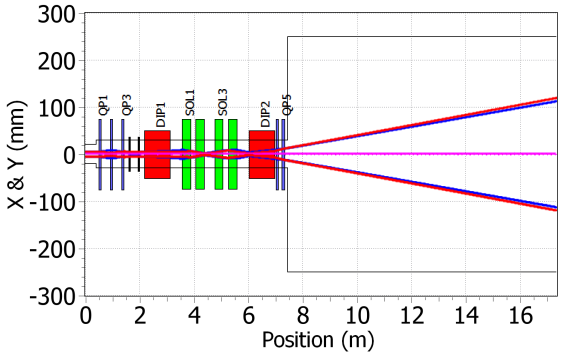

Figure 6: 3-σ rms transverse size from the end of the HWR section up the beam dump.

Dump Line-1

The Dump line-1 is necessary for extracting the beam from the hot standby injector. This line consists in a bending section and an expander one. The bending section utilizes the same achromatic design as MEBT-2. The expander consists of a double quadrupole, followed by a drift space of 10 m, which helps to achieve a symmetrically large transverse beam and maintain a relatively low peak power density at the dump entrance, as presented in Fig. 6. Table 3 lists the parameters of the main elements of Dump line-1.

Table 3: Main parameters of the Dump line-1. DIP stands for double switch dipole, SOL for solenoid, and QP for quadrupole.

Element	length (mm)	Magnet Gradient (T/m) / Voltage (kV) / Field (T)
DIP1 & DIP2	942	0.5
SOL1 & SOL4	300	2.9
SOL2 & SOL3	300	-2.8
QP4	100	3.4
QP5	100	-3.1

MULTIPARTICLE SIMULATIONS RESULTS

Multiparticle simulations were conducted using a step-by-step approach. Since there is no commercially available program that can accurately simulate all sections of an accelerator, beam extraction was carried out using AXCEL-INP 2-D [13], a Vlasov solver designed for axisymmetric and planar steady-state systems. Figure 7 illustrates the triode extraction system along with the extracted beam.

The dynamics of the LEBT were simulated using the Warp [14] and TraceWin [15] codes. Initially, TraceWin was employed to simulate the LEBT in a steady state [6]. Later, Warp was selected for studies involving transient effects and self-consistent space charge compensation of the beam [7,8], as shown in Fig. 8.

The RFQ reference design was developed using the RFQuick design code [10]. Figure 9 presents the horizontal

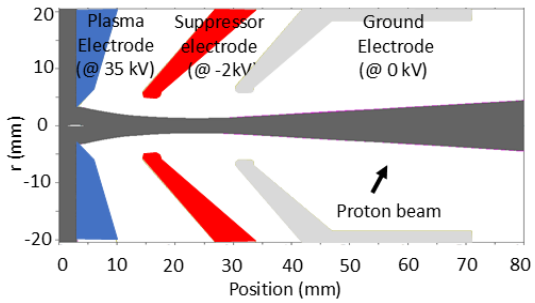

Figure 7: Beam extracted for the triode extraction systems for the JAEA-ADS.

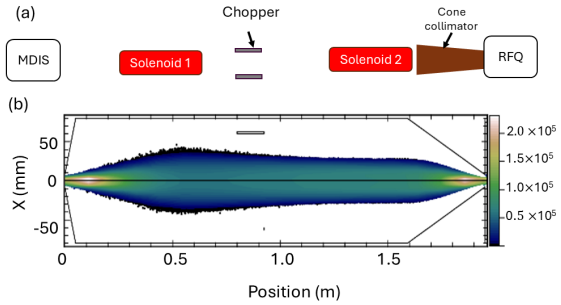

Figure 8: Schematic of the LEBT (a) and horizontal beam distribution after reached the steady-state in Warp simulations (b).

distribution along the RFQ. The RFQ's transmittance was 97%.

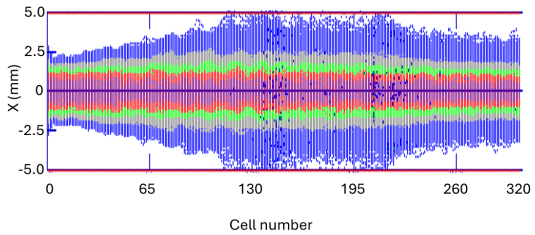

Figure 9: Horizontal distribution along the RFQ.

For the downstream simulations, TraceWin was used. The transverse envelopes and beam length for 3-σ are displayed in Fig. 10, from the entrance of the MEBT to the end of the first SSR1 cavity section.

Figure 11 shows both the input and output distributions employed in the analysis. Although no additional beam losses were observed, an noticeable emittance growth in the MEBT-2 section of 35% occurred, as presented in Fig. 12.

The Dump line-1 efficiently transports the beam to the dump entrance without any losses. The beam distribution at the dump (Fig. 13) shows a rms size of 38 mm. With a beam power of 1.7 kW and a conical collimator in place, we estimated the peak power density using the following formula [16]:

$$P_{max} = \frac{PA}{4\pi\sigma^2 L}, \qquad (1)$$

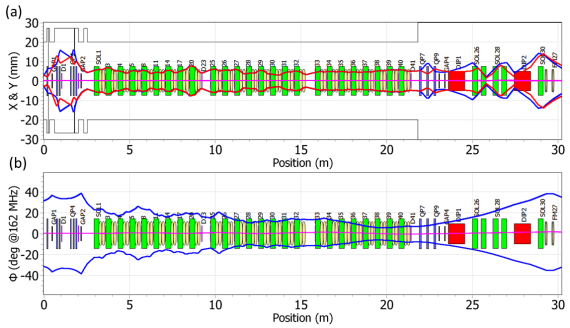

Figure 10: Transverse size (a) and bunch length (b) from the MEBT to the first period of the SSR1 section.

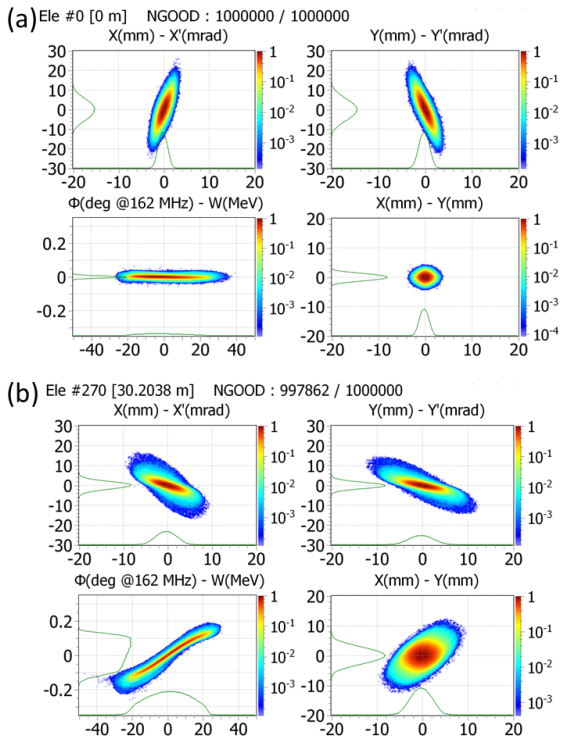

Figure 11: Initial distribution at the entrance of the MEBT (a) and final distribution (b) at the end of the first period of the SSR1 section.

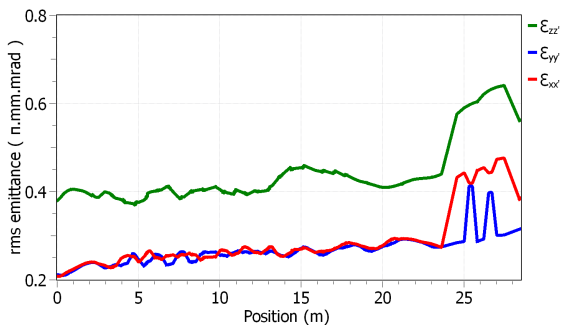

Figure 12: Rms emittance from the MEBT to the end of MEBT-2.

where P is the beam power, A, aperture of the dump, σ, rms size of the beam, and L, length of the cone. The dump's aperture is 500 mm, and for a 1-m long conical dump, the P_{max} is 4.8 W/cm^2, which is approximately two orders of magnitude lower than current high-power dumps. A thermal analysis will be performed for a more accurate estimation of the peak values.

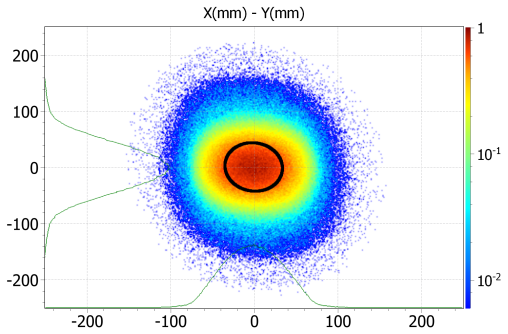

Figure 13: Transverse size at the entrance at the dump. The black curve shows the rms size that is about 38 mm in both planes.

CONCLUSIONS

To achieve a high-availability operation in the ADS linac, JAEA proposes implementing hot standby redundancy from the particle source to the HWR section, in this work it is referred to as the injector part.

Hot standby operation introduces new challenges in transporting the beam from the low-energy part to the high-energy one. Additionally, it imposes requirements of transverse space between the injectors for shielding and high-power beam dumps.

A double achromatic design facilitates beam transport to the high-energy section or the beam dump. Furthermore, using a pulse mode for the hot standby part reduces beam power dump, simplifying the dump design.

The current injector design meets the requirements of zero beam loss, sufficient shielding space over 5.4 m, and acceptable low peak power density of 4.8 W/cm^2 and integral power of 1.7 kW in the dump.

Future studies will explore the reduction of the emittance growth by optimization of the lattices.

ACKNOWLEDGMENTS

The authors would like to thank to the members of the JAEA-ADS group for their comments and suggestions. This work is supported by JSPS KAKENHI Grant Number 24H00235.

REFERENCES

[1] T. Sugawara *et al.*, "Research and Development Activities for Accelerator-Driven System in Jaea", *Prog. Nucl. Energy*, vol. 106, p. 27, Feb. 2018. doi:10.1016/j.pnucene.2018.02.007

[2] H. Takei *et al.*, "Estimation of acceptable beam-trip frequencies of accelerators for accelerator-driven systems and comparison with existing performance data", *J. Nucl. Sci. Techol.*, vol. 49, p. 384, Sep. 2012. doi:10.1088/00223131.2012.669239

[3] B. Yee-Rendon *et al.*, "Beam dynamics studies for fast beam trip recovery of the Japan Atomic Energy Agency accelerator-driven subcritical system", *Phys. Rev. Accel. Beams.*, vol. 25, p. 080101, Dec. 2022. doi:10.1103/PhysRevAccelBeams.25.080101

[4] B. Yee-Rendon *et al.*, "Design and beam dynamic studies of a 30-MW superconducting linac for an accelerator-driven subcritical system", *Phys. Rev. Accel. Beams.*, vol. 24, p. 120101, Dec. 2021. doi:10.1103/PhysRevAccelBeams.24.120101

[5] B. Yee-Rendon *et al.*, "Design and Optimization of a Proton Source Extraction System for the JAEA-ADS Linac", in *Proc. of the IPAC2023*, Venezia, Italy, May. 2023, TUPA121, pp. 1573-1575.

[6] B. Yee-Rendon *et al.*, "Design of the Low Energy Beam Transport Line for the JAEA-ADS Linac", in *Proc. of the PASJ2023*, Funabashi, Japan, Aug. 2023, WEP23, pp. 545-549.

[7] B. Yee-Rendon *et al.*, "Design and Beam Dynamics Studies of a Chopper for the JAEA-ADS LEBT", in *Proc. of the PASJ2024*, Yamagata, Japan, Jul. 2024, WEP001, pp. 488-491.

[8] B. Yee-Rendon *et al.*, "Beam Transient Studies for the JAEA-ADS LEBT", in *Proc. of the LINAC2024*, Chicago, USA, Aug. 2024, TUPB076, pp. 205-209.

[9] Y. Kondo *et al.*, "Reference design of the RFQ for JAEA-ADS linac", *JPS. Conf. Proc.*, vol. 33, p. 011015, March 2021. doi:10.7566/JPSCP.33.011015

[10] K. R. Crandall *et al.*, "RFQ design codes", LANL, Los Alamos, USA, Tech. Rep. LA-UR-96-1836 Revised December 7, 2005.

[11] E. Traykov *et al.*, "Double Achromat Solution with a Dedicated Collimation System for the MEBT-3 Section of MYRRHA", in *Proc. of the IPAC2023*, Venezia, Italy, May. 2023, MOPA004, pp. 63-65.

[12] Z. Guo *et al.*, "A Local Achromatic Design of the C-ADS MEBT2", in *Proc. of the IPAC2013*, Shanghai, China, May 2013, TUPWO019, pp. 1922-1924.

[13] *AXCEL-INP USER MANUAL*, INP, Germany, Mar. 2012, pp. 24–43.

[14] A. Friedman *et al.*, "Computational methods in the WARP code framework for kinetic simulations of particle beams and plasmas", *IEEE Trans. Plasma Sci.*, vol. 42, p. 1321, June 2013. doi:10.1109/PLASMA.2013.6633427

[15] TraceWin Manual, http://irfu.cea.fr/dacm/logiciels

[16] H. Jia *et al.*, "Design and Development of the 200-kW Beam Dump", *Nucl. Sci. and Eng.*, vol. 1981(1), p. 64, Jan 2024. doi:10.1080/00295639.2022.2164149